

Diffuse single-crystal scattering corrected for molecular form factor effects

Ella Schmidt* and Reinhard B. Neder

Lehrstuhl für Kristallografie und Strukturphysik, Friedrich-Alexander-Universität Erlangen–Nürnberg, Staudtstrasse 3, 91058 Erlangen, Germany. *Correspondence e-mail: ella.schmidt@fau.de

Received 27 October 2016

Accepted 10 February 2017

Edited by D. A. Keen, STFC Rutherford Appleton Laboratory, UK

Keywords: diffuse scattering; molecular form factors.

This paper shows that chemical short-range order in two-component molecular crystals can be solved directly by separating the influence of the molecular form factor from the diffraction pattern. This novel technique is demonstrated by analysing the diffuse scattering of tris-*tert*-butyl-1,3,5-benzene tricarboxamide.

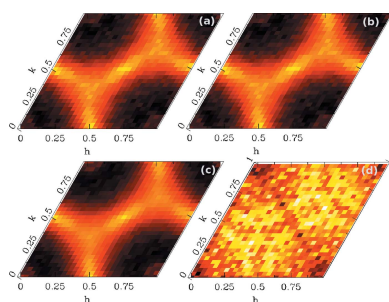
1. Introduction

The determination of the average structure of a crystalline material *via* analysis of Bragg scattering data has long since become a routine method, at least for materials with moderate complexity. No technique equivalent to direct methods has been established to date for the analysis of disordered crystalline materials. If disorder is present in a crystalline material, however, the data analysis is still not straightforward. For a full analysis the information contained in the weaker diffuse scattering between the Bragg peaks is needed.

Numerous different types of disorder exist; see Welberry & Weber (2015) for a recent review. Strictly speaking, any deviation from a perfect average crystal structure will cause diffuse scattering. If the deviations are randomly distributed throughout the sample monotonic Laue scattering arises. If the defects in the sample show a tendency to order, which is not periodic but restricted to an approximate order, usually referred to as short-range order (SRO), the resulting diffuse scattering becomes modulated throughout reciprocal space. The deviations from the perfect crystal structure can be of occupational or displacive type, or a combination of both. Stacking faults (Welberry, 1985), density waves (Neder & Proffen, 2008) and chemical SRO in alloys (Welberry & Butler, 1995) are examples of occupational disorder. The most common type of displacement disorder is thermal motion (Debye, 1913), but displacement waves (Neder & Proffen, 2008) caused by phonons or size effects (Warren *et al.*, 1951) resulting in displacement because of chemical SRO can also be considered as displacement disorder.

Many different approaches for the interpretation of diffuse scattering data exist (see Welberry & Weber, 2015). For most disordered structures solved so far a unique approach was taken and a specific model was developed. No standard algorithm has been established to solve any arbitrary disordered structure.

In the first half of the 20th century analytical equations were developed to describe the diffuse scattering due to thermal motion (Debye, 1913), chemical SRO (Laue, 1918) and resulting size effects (Warren *et al.*, 1951). A summary of the analytically derived models can be found in the books of



Warren (1990), Welberry & Butler (1994), Krivoglaz (1996) and Nield & Keen (2001).

The theoretical equations for diffuse scattering have been widely applied in the field of stacking faults and SRO in binary metal alloys; a more complete list of examples can be found in Welberry & Weber (2015). Reinhard *et al.* (1990) solved the chemical SRO in α -brass by fitting analytical equations to the measured diffuse scattering. A more recent example discussing stacking faults can be found in Bürgi *et al.* (2005). A combination of first-order diffuse scattering due to chemical SRO and the resulting size effect has been applied to metal alloys (Terauchi & Cohen, 1979; Morinaga & Cohen, 1979; Morinaga *et al.*, 1980). A more recent example can be found in Schönfeld *et al.* (2011). Wehinger *et al.* (2014) recently used theoretical equations to interpret thermal diffuse scattering of ice. Withers discusses the application of symmetry analysis in terms of a group-theoretical approach for diffuse electron diffraction (Withers *et al.*, 2010; Withers, 2015).

With the advancement of computational power Monte Carlo methods were established to model diffuse scattering (Welberry & Butler, 1994; Proffen & Welberry, 1997*b*; Neder & Proffen, 2008). The direct Monte Carlo method requires an initial disorder model. The corresponding disorder parameters can then be refined against the diffuse scattering data. Reverse Monte Carlo (RMC) (McGreevy & Pusztai, 1988) modelling, on the contrary, starts with an arbitrary start structure. The structure is modified by changes that may include moving individual atoms or molecules or switching the positions of atom/molecule pairs. The resulting structure must be analysed after the RMC process has finished, *i.e.* once the calculated and experimentally observed scattering diffraction patterns match well enough. The approach has the advantage that no initial model must be known and has been applied mostly to powder diffraction data (Keen *et al.*, 1990, 2007; Tucker *et al.*, 2000, 2005; Cliffe *et al.*, 2010). Since the structural model will consist of a few tens of thousands of atoms, many conformations may match the experimental diffraction pattern. Especially for powder diffraction data, suitable constraints are usually required to obtain a meaningful solution. Even for single-crystal data that are refined without constraints, unphysical interatomic distances are likely to be generated (Proffen & Welberry, 1997*a*).

More recently, the three-dimensional delta pair distribution function (3D- Δ PDF) (Weber & Simonov, 2012) has been established for the analysis of diffuse scattering. For this technique the experimental diffuse scattering is separated from Bragg scattering, and the Fourier transform of this purely diffuse scattering yields the 3D- Δ PDF. The 3D- Δ PDF thus contains information on the deviation of the local structure from the average crystal structure. The method allows for extensive, fast and fairly general modelling of diffuse scattering (Simonov, 2014; Simonov *et al.*, 2014*a,b*; Urban *et al.*, 2015). The technique depends on the measurement of a complete three-dimensional scattering data set. The Bragg data have to be removed from the experimental data and therefore the method works best if the diffuse scattering is well separated from the Bragg reflections.

In this paper we present a technique to separate the influence of a molecular form factor from the diffuse scattering intensity. As the data are treated in reciprocal space only, the method is less susceptible to incomplete data sets than *e.g.* the 3D- Δ PDF.

2. Theoretical model for short-range order

In general, a disordered crystal structure can be described as an average structure plus local deviations. These local deviations may be of substitutional and/or of displacive type. Individual atoms and/or molecules or even small clusters of the average structure may be substituted by other atoms or molecules, or be shifted from the average position. The average crystal structure manifests itself in the Bragg intensities, while the local deviations and particularly the correlations between the local deviations cause the diffuse scattering.

The present model is restricted to the analysis of crystalline compounds with substitutional SRO. This restriction simplifies the diffuse scattering equations tremendously. Pure displacement disorder and the general combination of substitutional and displacement disorder will be treated in separate communications.

The model is applicable to structures that consist of individual atoms as well as molecular compounds. Its main benefit lies in the analysis of the diffuse scattering of molecular compounds, as the molecular form factor modifies the diffuse scattering signal.

Here we consider a simple two-component molecular crystal system, where no displacement disorder is present. This is for example the case for molecular crystals, where the base molecule exists in two conformations. It is likely that the two conformations exhibit SRO in a crystal, but since they are chemically identical, a size effect may be neglected. This is *e.g.* the case for tris-*tert*-butyl-1,3,5-benzene tricarboxamide, analysed with 3D- Δ PDF in Simonov *et al.* (2014*b*).

2.1. Analytical equation for short-range order

The theoretical development of equations to describe diffuse scattering in a correlation-wave approach can be found in Warren *et al.* (1951). Analogous equations are used *e.g.* by Welberry & Butler (1994), Welberry (2004), Weber & Simonov (2012) and Chodkiewicz *et al.* (2016):

$$I_{\text{SRO}}(h_1 h_2 h_3) = N m_A m_B |f_B - f_A|^2 \left[1 + \sum_{lmn} \alpha_{lmn} \cos(2\pi(h_1 l + h_2 m + h_3 n)) \right]. \quad (1)$$

Here I_{SRO} is the diffuse intensity due to SRO, which is a function of the reciprocal-space coordinates h_1 , h_2 and h_3 . The crystal consists of N atoms/molecules of species A and B . m_A , m_B and f_A , f_B are the respective concentrations and atomic/molecular form factors of the species. The summation over lmn is a summation over all interatomic vectors and the α_{lmn} are the Warren–Cowley SRO parameters.

Any further atoms or molecules in the structure that are not affected by SRO do not contribute to equation (1), only to the

Bragg reflections. These atoms do not affect the derivation in this paper.

Equation (1) consists of two nontrivial factors. $|f_B - f_A|^2$ is the squared form factor difference between the two components involved in the SRO. As the form factor difference corresponds to that of a single atom/molecule pair, its contribution in reciprocal space is a continuous, smoothly varying intensity distribution. It depends on the respective molecular structures and is not related to the SRO intensity distribution.

The last term in equation (1) in the square brackets expresses the diffuse scattering by an SRO distribution of point scatterers. For a structure with a primitive unit cell and one disordered species per unit cell, the contribution by the defect distribution is periodic in reciprocal space. Depending on the correlations between neighbouring defects this contribution by itself will cause a periodic pattern of diffuse peaks or lines.

2.2. Application to data

The two components of equation (1) are multiplied to give the diffuse scattering intensity due to chemical SRO. The multiplication of the two independent components may severely obscure the underlying pure SRO diffuse scattering. Fig. 1(a) shows part of the diffuse scattering for tris-*tert*-butyl-1,3,5-benzene tricarboxamide (Simonov *et al.*, 2014b) to be compared with the pure, periodic disorder diffuse scattering in Fig. 1(d). The molecular components *A* and *B* are shown in Fig. 2.

This multiplication of the disorder diffuse intensity with the squared molecular form factor difference prevents a direct determination of the underlying disorder model. Once a suitable model has been found, it is straightforward to calcu-

late the diffuse scattering as a product of the two terms. Weber *et al.* (2001) used the influence of the molecular form factor on the diffuse scattering to distinguish contributions from the host and guest molecules in an inclusion compound. Chodkiewicz *et al.* (2016) used the form factor difference squared to improve the average structure model. A similar approach to handling diffuse scattering has been utilized in *DISCUS* to calculate the diffuse scattering from a distribution of layers in stacked materials (Neder & Proffen, 2008).

Equation (1) consists of a simple product of the disorder diffuse scattering contribution and the squared molecular form factor difference. Dividing the experimental diffuse scattering data by this difference decouples the influence of the molecular form factors and results in a quantity that is directly connected to the SRO parameters α_{lmn} . Regions where the molecular form factor difference is approximately zero have to be excluded from the division. This is further discussed below.

The resulting pattern consists of periodic diffuse maxima. The cosine series in equation (1) is periodic in reciprocal space with periodicity $h_1l + h_2m + h_3n$. For simple structures with primitive unit cells, or structures where only one component of a more complex unit cell is involved in the SRO, the interatomic vectors between the short-range-ordered components are multiples of the base vectors **a**, **b** and **c**; hence *l*, *m* and *n* are integers. In the summation in equation (1) the maximum periodicity length involved corresponds to one reciprocal unit cell. Therefore, after the division of the experimentally obtained scattering pattern by the absolute form factor difference squared, the information contained in every reciprocal unit cell is equivalent. The approach for data treatment suggested here is the projection of all intensities into one reciprocal unit cell and the consecutive fitting of the cosine series weighted with the α_{lmn} .

As the cosine series in equation (1) is a linear function of α_{lmn} , the analysis can be performed by a simple linear least-squares fit. Such a linear least-squares refinement does not require prior knowledge of approximately correct starting values. Thus, the SRO parameters are accessible directly, eliminating the need to find a good starting model and the disorder model of such systems can be solved directly.

The cosine series in equation (1) can also be interpreted as a Fourier series. Thus, a discrete Fourier transform will immediately give the SRO parameters as well. The first Fourier coefficient corresponds to the scale factor, for all other coefficients are related to the SRO parameters as $f_{lmn} = \alpha_{lmn}f_{000}$.

We prefer to use the linear regression instead of the Fourier transform. In case the data set is incomplete, *e.g.* there are pixels in the projected reciprocal unit cell that are left empty, a linear regression can simply exclude these data points, while an analysis utilizing a Fourier transform becomes much more difficult.

For the example discussed in the following, tris-*tert*-butyl-1,3,5-benzene tricarboxamide, the average crystal structure was solved beforehand (Kristiansen *et al.*, 1997). The average structure clearly suggested two molecular components *A* and *B*. Therefore, the absolute form factor difference squared

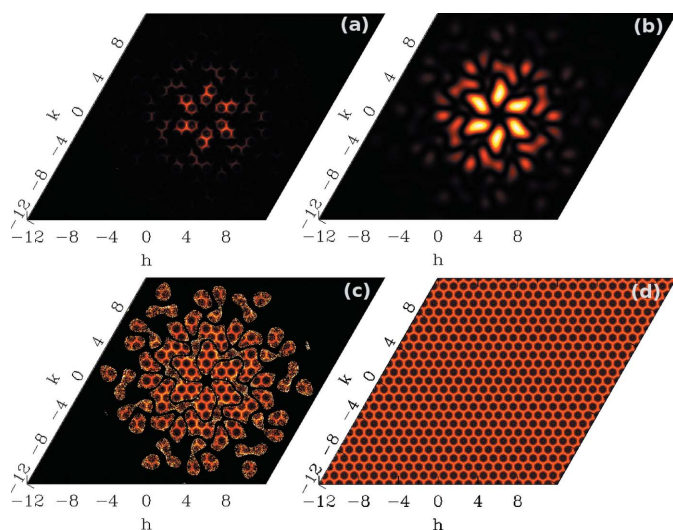


Figure 1
(a) Experimentally obtained diffuse scattering of tris-*tert*-butyl-1,3,5-benzene tricarboxamide in the (*hk*1) plane. (b) Absolute molecular form factor difference squared in the (*hk*1) plane. (c) Result of division. For details see text. The intensity scale is the same as for (a). (d) Calculated diffuse intensity with the SRO parameters given in Table 1.

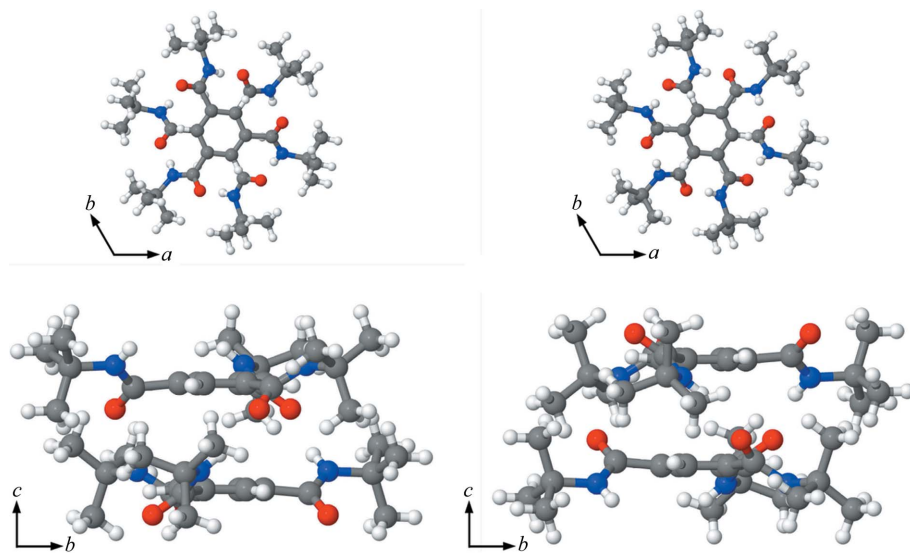


Figure 2

Example of molecular stacks *A* and *B*. The molecules within a stack are linked with a helical system of hydrogen bonds. In stacks of type *A* the O atoms point downwards, while in stacks of type *B* the O atoms point upwards.

could be calculated accurately. The division of the experimental data by the absolute form factor difference squared could be performed straightforwardly but with caution: experimental data are always affected by noise. At points in reciprocal space, where $|f_B - f_A|^2$ is very small, the diffuse scattering will also be very small. These points have to be masked prior to the division and consecutive data analysis, otherwise the division process may over-amplify the noise, which would lead to unphysical results. For data where the relative accuracy of each pixel is known, a weighted projection scheme should be used, to further reduce the influence of noise.

Disordered structures are often refined using split positions. This sometimes results in overlapping atomic positions and makes a distinction into separate molecular species very difficult or even impossible. If a molecule is located at one site in two slightly different orientations, it is for example not straightforward to assign disordered side groups unambiguously. The projection technique described above provides a tool to overcome such difficulties and access SRO directly. As long as the atomic species and their occupancies in the molecular components involved in the ordering are known (this should be possible for all compounds by chemical analysis) the average atomic form factor can be calculated.

Dividing the experimentally obtained scattering pattern by this average form factor annihilates the characteristic decrease of scattering intensity with increasing distance from the origin in reciprocal space. Possibly, a further correction for thermal motion has to be applied in the form of a Debye–Waller factor. A consecutive projection of the data into one reciprocal unit cell will also give a reasonable estimate of the SRO parameters: since the absolute molecular form factor difference squared is a smoothly varying function in reciprocal space, a projection of the absolute molecular form factor difference squared into one reciprocal unit cell gives a reasonably flat

function (see *e.g.* Fig. 3*d*). Hence, the modulation in the projected experimentally obtained intensity pattern is predominantly due to chemical SRO. The SRO parameters α_{lmn} can be accessed by the same linear regression as for the case with the known absolute molecular form factor difference squared. Again, if the relative accuracy of the data used is known, we suggest using a weighted projection scheme.

The evaluation of SRO parameters without prior knowledge of the average crystal structure opens up new possibilities. As described in Chodkiewicz *et al.* (2016) the average crystal structure can be refined on the diffuse scattering, when the SRO parameters are known. For structure refinements similar to those in Chodkiewicz *et al.* (2016) we suggest first applying the projection technique described here to obtain the

SRO parameters and then refining the average molecular structure using the absolute form factor difference squared as in Chodkiewicz *et al.* (2016).

Another possible application of the projection technique is short-range-ordered inclusion compounds. Inclusion compounds, like the urea inclusion compounds discussed in ch. 10 of Welberry (2004), consist of a host lattice and guest molecules. Both the host lattice molecules and the guest molecules can exhibit SRO, which manifests itself in diffuse scattering. In the case of a short-range-ordered host lattice, a projection of the diffuse intensity into one reciprocal unit cell is very likely to average out the diffuse contributions of the guest molecules and in this manner the SRO of the host lattice can be analysed separately, dramatically simplifying the consecutive analysis of the diffuse scattering due to the SRO of the guest molecules.

3. Experimental demonstration

The procedure for treating diffuse scattering of binary molecular systems as described above is demonstrated by applying it to the diffuse scattering of tris-*tert*-butyl-1,3,5-benzene tricarboxamide. The data were taken from Simonov *et al.* (2014*b*) with kind permission.

3.1. Data analysis for known average structure

Tris-*tert*-butyl-1,3,5-benzene tricarboxamide crystallizes in $P6_3/m$. The average crystal structure consists of a columnar packing along the *c* axis with one column per unit cell. An individual molecule does not possess mirror symmetry and the crystal consists of columns of two enantiomers. Within a column, the 6_3 axis forms perfectly periodic stacks along *c*. Details about the molecular arrangement can be found in Simonov *et al.* (2014*b*) and in Fig. 2. The disorder within the

structure was analysed successfully via the 3D- Δ PDF technique. The analysis showed that the diffuse scattering is very well described by a model with negative correlations between neighbouring columns. Given the overall hexagonal symmetry this results in a locally frustrated alternation of 'up' and 'down' pairs. Such a disorder produces very characteristic, almost honeycomb-like diffuse scattering, which is just partially visible in Fig. 1(a).

The underlying crystal and molecular symmetry suggests that the α_{lmn} are equivalent for symmetry-equivalent lmn , e.g. due to the sixfold symmetry axis α_{100} , α_{010} , α_{110} , $\alpha_{\bar{1}00}$, $\alpha_{\bar{1}10}$ and $\alpha_{\bar{1}\bar{1}0}$ are equivalent.

Projected along the c axis all columns are identical; therefore the form factor difference is zero in the $(hk0)$ plane. Accordingly, no diffuse scattering was observed in this plane. The diffuse scattering is restricted to (hkl) planes with integer l . The strongest diffuse scattering is observed in the $(hk1)$ plane shown in Fig. 1(a).

The squared form factor difference between an 'up' and 'down' molecule was calculated using the average crystal structure of the 'up' and 'down' conformation of the molecule, with the program *DISCUS* (Proffen & Neder, 1997). The result is shown in Fig. 1(b). For the division procedure the absolute form factor difference squared is normalized with respect to its maximum value. Points in reciprocal space, where the resulting intensity is less than 0.01 of the maximum value, are excluded from the division and model refinement. Fig. 1(c) shows the result of the division. The intensity scale is identical to that in (a). The division clearly enhances the honeycomb pattern in the unmasked areas.

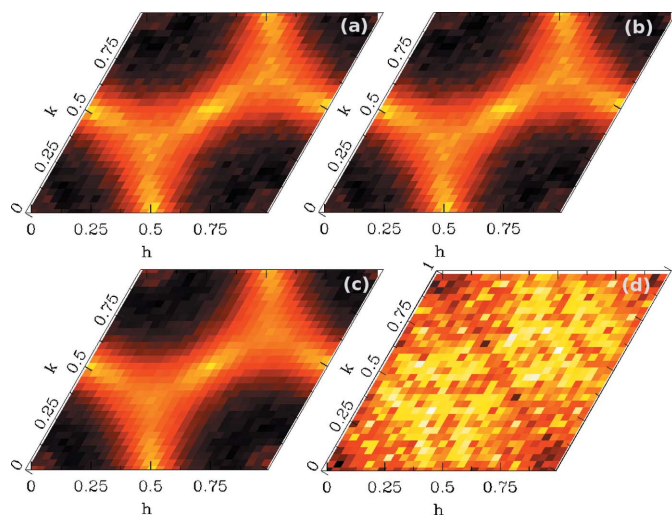


Figure 3

(a) Projection of the experimental data into one reciprocal unit cell after division by the absolute molecular form factor difference squared. (b) Diffuse intensity calculated from the parameters given in Table 1. The colour scale is the same as for (a). (c) Projection of the experimental data into one reciprocal unit cell after division by the average atomic form factor squared. (d) Projected absolute molecular form factor difference squared. The ratio between the minimum and maximum intensity shown is 1.002; hence the projected intensity is reasonably flat. The colour scheme was chosen to show all differences that still exist. The relative difference between minimum and maximum intensity is three orders of magnitude less compared with the other figures, where SRO is present.

Table 1

Refined SRO parameters: comparison of refinement with *YELL* and the linear regression described here.

SRO parameter	<i>YELL</i>	Division by $ f_B - f_A ^2$ and projection	Division by $ f_{\text{aver}} ^2$ and projection
100	-0.25157 (7)	-0.22794	-0.22122
200	0.09841 (6)	0.09597	0.10417
210	0.09500 (6)	0.10026	0.10333
300	-0.03448 (6)	-0.02499	-0.02175
310	-0.05324 (6)	-0.03902	-0.03300
320	-0.04348 (6)	-0.04056	-0.03943
400	0.01637 (6)	0.01827	0.01556
410	0.02556 (6)	0.01738	0.02112
420	0.03100 (6)	0.03138	0.03315
430	0.01650 (6)	0.02351	0.02252
500	-0.00898 (6)	-0.00608	-0.00441
510	-0.01283 (6)	-0.00351	-0.00459
520	-0.01747 (6)	-0.00141	-0.01477
530	-0.01487 (6)	-0.00140	-0.01099
540	-0.00731 (6)	-0.00883	-0.00693
600	0.00669 (6)	0.00475	0.00176
610	0.00625 (6)	0.00156	0.00222
620	0.01014 (6)	0.00097	0.00358
630	0.00832 (6)	0.00551	0.00748
640	0.00797 (6)	0.00630	0.00686
650	0.00356 (6)	0.00146	0.00570
700	-0.00359 (6)	0.00024	-0.00045
710	-0.00424 (6)	-0.00599	-0.00463
720	-0.00583 (6)	-0.00229	-0.00107
730	-0.00622 (6)	-0.00881	-0.00469
740	-0.00591 (6)	-0.00499	-0.00405
750	-0.00257 (6)	-0.01078	-0.00541
760	-0.00333 (6)	-0.00029	-0.00315

The result of the division shown in Fig. 1(c) is projected into one reciprocal unit cell. Because of the masking, a counting algorithm is implemented, during the projection. For every point in the reciprocal unit cell, the number of data points projected onto this point is counted and the projected intensity is normalized by this count rate. The result of the projection is shown in Fig. 3(a). The relative accuracy of the data used here is not known; therefore a projection scheme with unit weights was used.

The data resolution predetermines the resolution of the projection; in the case here the projected unit cell is 30×30 pixels. Data were kindly provided for all reciprocal layers $(hk-6)$ to $(hk5)$ plane and all layers were used in our analysis. The only layer excluded is $(hk0)$, since here the squared form factor difference is zero. This added up to a total of 2 822 087 data points that were projected onto 900 data points in one reciprocal unit cell. The projected intensity is analysed with a direct refinement of $c[1 + \sum_{lmn} \alpha_{lmn} \cos(2\pi(h_1l + h_2m + h_3n))]$, where c is a scale factor refined during the fit.

Analogous to the analysis in Simonov *et al.* (2014b), the first seven shells of SRO parameters α_{lmn} were refined with a linear regression analysis, which results in 28 refined SRO parameters. The SRO diffuse scattering calculated from the refined SRO parameters is shown in Fig. 3(b). The model and the data agree very well; the refined R value of the projected data and the calculated model is 3.8%. The refinement of the projected intensity is done within seconds on a regular desktop computer.

The final SRO parameters are listed in Table 1 and compared with the results of an equivalent refinement of the data that we carried out with *YELL* (Simonov *et al.*, 2014a). *YELL* performs a 3D- Δ PDF calculation. Consistent with the data analysis by division, the first seven shells of SRO parameters α_{lmn} were left as fit parameters. *YELL* was only allowed to fit SRO to the calculated 3D- Δ PDF and no other type of disorder. As *DISCUS* (used for the calculation of $|f_B - f_A|^2$) currently uses isotropic atomic displacement parameters, the refinement with *YELL* was performed with isotropic atomic displacement parameters as well. The *R* value *YELL* achieved for this refinement is 29.5%. The difference in *R* values from *YELL* (29.5%) and the linear least-squares algorithm (3.8%) used here can be explained by the size of the data set: the projection algorithm averages out statistical errors, which contribute to the *R* value when the whole data set is fitted, which is done in *YELL*.

The agreement between the SRO parameters obtained from our direct analysis of the divided and projected diffuse scattering and the parameters obtained through *YELL* is excellent even to the outer shells. The data were also analysed using a discrete Fourier transformation of the projected data. The results of the Fourier transformation are up to the third decimal place or more identical with the results of the linear regression.

3.2. Data analysis for unknown average structure

As a proof of concept, we performed the data analysis on the same structure but as though the average structure was unknown. Tris-*tert*-butyl-1,3,5-benzene tricarboxamide has the chemical formula $C_{21}H_{33}N_3O_3$, which can be known from chemical analysis. This is enough information to calculate the average atomic form factor squared of the atoms involved in the diffuse scattering. The data obtained in the experiment are divided by this average form factor squared to correct for the systematic decay of the diffracted intensity in reciprocal space with increasing h .

The resulting intensity was projected into one reciprocal unit cell as described above, which is shown in Fig. 3(c). The same resolution of 30×30 pixels is present. As a proof of principle, the absolute form factor difference squared was also projected into one reciprocal unit cell, which is shown in Fig. 3(d). The resulting function is reasonably flat. The ratio between the maximum and minimum intensity of the projected absolute form factor difference squared is 1.002.

The projected experimental intensity was fitted in the same manner as above for the known average structure. The fitting results for the refined SRO parameters are shown in Table 1, and agree very well with the parameters obtained from *YELL* and the same procedure with the known average structure. The *R* value of the fit is 4.4%. This result clearly shows that SRO parameters are accessible directly from diffuse scattering without prior knowledge of the average structure involved. The technique presented here therefore enables access to the SRO parameters involved in a wide variety of disordered molecular compounds.

4. Conclusion

We have demonstrated a novel technique to access chemical SRO in disordered binary molecular systems. The influence of the molecular form factor on the diffuse scattering is decoupled which implies the SRO parameters can be accessed directly. The division process described above clearly modifies the diffuse scattering in such a way that the underlying SRO diffuse scattering becomes much easier to recognize. The modulations of the diffuse scattering due to the molecular form factors are effectively suppressed.

The projection approach described above enables a direct access to SRO parameters, even when the average crystal structure is not known or only partly known. This makes the approach described here a powerful tool that can be applied to a wide variety of disordered materials.

Another advantage of the technique demonstrated above lies in its ability to deal with incomplete data sets. The projection does not need a complete three-dimensional data set: as long as enough data points are provided, so that for every pixel in the projected unit cell a statistical average can be formed during projection, the technique described gives access to the SRO parameters.

Acknowledgements

The kind permission of Thomas Weber to use the original data for our analysis is gratefully acknowledged.

References

- Bürgi, H.-B., Hostettler, M., Birkedal, H. & Schwarzenbach, D. (2005). *Z. Kristallogr.* **220**, 1066–1075.
- Chodkiewicz, M. L., Makal, A., Gajda, R., Vidovic, D. & Woźniak, K. (2016). *Acta Cryst.* **B72**, 571–583.
- Cliffe, M. J., Dove, M. T., Drabold, D. A. & Goodwin, A. L. (2010). *Phys. Rev. Lett.* **104**, 125501.
- Debye, P. (1913). *Ann. Phys.* **348**, 49–92.
- Keen, D. A., Goodwin, A. L., Tucker, M. G., Dove, M. T., Evans, J. S. O., Crichton, W. A. & Brunelli, M. (2007). *Phys. Rev. Lett.* **98**, 225501.
- Keen, D. A., Hayes, W. & McGreevy, L. (1990). *J. Phys. Condens. Matter*, **2**, 2773–2786.
- Kristiansen, M., Smith, P., Chanzy, H., Baerlocher, C., Gramlich, V., McCusker, L., Weber, T., Pattison, P., Blomenhofer, M. & Schmidt, H.-W. (1997). *Cryst. Growth Des.* **9**, 2556–2558.
- Krivoglaz, M. A. (1996). *Diffuse Scattering of X-rays and Neutrons by Fluctuations*. Berlin, Heidelberg: Springer-Verlag.
- Laue, M. V. (1918). *Ann. Phys.* **361**, 497–506.
- McGreevy, R. L. & Pusztai, L. (1988). *Mol. Simul.* **1**, 359–367.
- Morinaga, M. & Cohen, J. B. (1979). *Acta Cryst.* **A35**, 975–989.
- Morinaga, M., Cohen, J. B. & Faber, J. (1980). *Acta Cryst.* **A36**, 520–530.
- Neder, R. B. & Proffen, T. (2008). *Diffuse Scattering and Defect Structure Simulations: a Cook Book Using the Program DISCUS*. Oxford University Press.
- Nield, V. M. & Keen, D. A. (2001). *Diffuse Neutron Scattering from Crystalline Materials*. Oxford: Clarendon Press.
- Proffen, Th. & Neder, R. B. (1997). *J. Appl. Cryst.* **30**, 171–175.
- Proffen, Th. & Welberry, T. R. (1997a). *Acta Cryst.* **A53**, 202–216.
- Proffen, T. & Welberry, T. R. (1997b). *Phase Transitions*, **67**, 373–397.
- Reinhard, L., Schönfeld, B., Kistorz, G. & Bührer, W. (1990). *Phys. Rev. B*, **41**, 1727–1734.
- Schönfeld, B., Sax, C. R. & Ruban, V. (2011). *Phys. Rev. B*, **85**, 014204.

- Simonov, A. (2014). PhD thesis, ETH Zürich, Switzerland.
- Simonov, A., Weber, T. & Steurer, W. (2014a). *J. Appl. Cryst.* **47**, 1146–1152.
- Simonov, A., Weber, T. & Steurer, W. (2014b). *J. Appl. Cryst.* **47**, 2011–2018.
- Terauchi, H. & Cohen, J. B. (1979). *Acta Cryst.* **A35**, 646–652.
- Tucker, M. G., Dove, M. T. & Keen, D. A. (2000). *J. Phys. Condens. Matter*, **12**, L723–L730.
- Tucker, M. G., Goodwin, A. L., Dove, M. T., Keen, D. A., Wells, S. A. & Evans, J. S. O. (2005). *Phys. Rev. Lett.* **95**, 255501.
- Urban, P., Simonov, A., Weber, T. & Oeckler, O. (2015). *J. Appl. Cryst.* **48**, 200–211.
- Warren, B. E. (1990). *X-ray Diffraction*. New York: Dover Publications.
- Warren, B. E., Averbach, B. L. & Roberts, B. W. (1951). *J. Appl. Phys.* **1493–1496**, 2–78.
- Weber, T., Estermann, M. A. & Bürgi, H.-B. (2001). *Acta Cryst.* **B57**, 579–590.
- Weber, T. & Simonov, A. (2012). *Z. Kristallogr.* **227**, 238–247.
- Wehinger, B., Chernyshov, D., Krisch, M., Bulat, S., Ezhov, V. & Bosak, A. (2014). *J. Phys. Condens. Matter*, **26**, 265401.
- Welberry, T. R. (1985). *Rep. Prog. Phys.* **48**, 1543–1594.
- Welberry, T. R. (2004). *Diffuse X-ray Scattering and Models of Disorder*. IUCr Monographs on Crystallography. Oxford University Press.
- Welberry, T. R. & Butler, B. D. (1994). *J. Appl. Cryst.* **27**, 205–231.
- Welberry, T. R. & Butler, B. D. (1995). *Chem. Rev.* **95**, 2369–2403.
- Welberry, T. R. & Weber, T. (2015). *Crystallogr. Rev.* **22**, 2–78.
- Withers, R. (2015). *IUCrJ*, **2**, 74–84.
- Withers, R. L., Aroyo, M. I., Perez-Mato, J. M. & Orobengoa, D. (2010). *Acta Cryst.* **B66**, 315–322.